Clump Detections and Limits on Moons in Jupiter's Ring System

Mark R. Showalter, *et al.*

Science **318**, 232 (2007);
DOI: 10.1126/science.1147647

Science (print ISSN 0036-8075; online ISSN 1095-9203) is published weekly, except the last week in December, by the American Association for the Advancement of Science, 1200 New York Avenue NW, Washington, DC 20005.

REPORT

Clump Detections and Limits on Moons in Jupiter's Ring System

Mark R. Showalter,[1*] Andrew F. Cheng,[2,3] Harold A. Weaver,[3] S. Alan Stern,[2] John R. Spencer,[4] Henry B. Throop,[4] Emma M. Birath,[4] Debi Rose,[5] Jeffrey M. Moore[6]

The dusty jovian ring system must be replenished continuously from embedded source bodies. The New Horizons spacecraft has performed a comprehensive search for kilometer-sized moons within the system, which might have revealed the larger members of this population. No new moons were found, however, indicating a sharp cutoff in the population of jovian bodies smaller than 8-kilometer-radius Adrastea. However, the search revealed two families of clumps in the main ring: one close pair and one cluster of three to five. All orbit within a brighter ringlet just interior to Adrastea. Their properties are very different from those of the few other clumpy rings known; the origin and nonrandom distribution of these features remain unexplained, but resonant confinement by Metis may play a role.

Planetary rings fall into two general categories: dense systems (exemplified by the main rings of Saturn) and faint, dusty rings (such as Jupiter's). The effects of plasma, electromagnetic perturbations, and solar radiation pressure limit the lifetimes of orbiting dust particles, so Jupiter's rings must be replenished continuously from a population of embedded "parent" bodies (*1*–*3*). Jupiter's moons Adrastea and Metis orbit within the main ring and are probably major sources of dust. However, spacecraft and Earth-based images have revealed a band of material ~1000 km wide between the orbits of the two moons (*3*–*5*); this is likely the primary source population.

We used the New Horizons spacecraft to search for small moons in the main ring during its Jupiter approach, to better understand the relationship between the parent population and the prevalent dust. Adrastea (mean radius r = 8 km, semimajor axis a = 128,981 km) and Metis (r = 22 km, a = 127,980 km) are the smallest known inner moons, but the Long-Range Reconnaissance Imager (LORRI) was capable of detecting bodies just 0.5 km in radius. A comprehensive search was accomplished via two image sequences or "movies," in which LORRI targeted one tip of the ring and snapped an image every 8 to 10 min for a full orbital period (7.2 hours). The two movies comprised 49 images (designated 34600923 to 34629723) and 63 images (34742163 to 34779663), respectively, and were separated by 1.3 days. Exposure times were 3 s; pointing instability contributed a few pixels of smear to most images.

A co-added image (Fig. 1A) clearly shows the 1000-km-wide ring between the orbits of the two moons. Peaks in brightness are visible interior to Adrastea and exterior to Metis. A third enhancement appears just outside the orbit of Adrastea. The moons themselves occupy local minima in ring density, but these regions are not empty. This same triple-peaked pattern was first imaged by the Galileo spacecraft (*3*) but with lower signal-to-noise ratio (SNR). This pattern describes the locations of parent bodies; the ring looks radically different at high phase angles (Sun-ring-observer angles) (Fig. 1, B and C), which emphasize the tiny dust particles in the system. Here, the finer structure disappears, and the main ring extends inward ~6000 km (*6*, *7*), indicating that the dust grains are dispersed primarily inward from their point of origin.

To search for new moons, we extracted a sequence of thin strips from each frame, in which polar coordinates in the ring plane were reprojected into a rectangular grid. Strips were generally 4000 km wide radially and were generated at overlapping 2000-km steps. Pixel resampling was 0.1° to 0.2° in longitude (horizontally) and 100 to 200 km radially (vertically). Strips from the same radial range of each movie frame were then stacked vertically into a single image. At this step, we rotated longitudes to a common epoch,

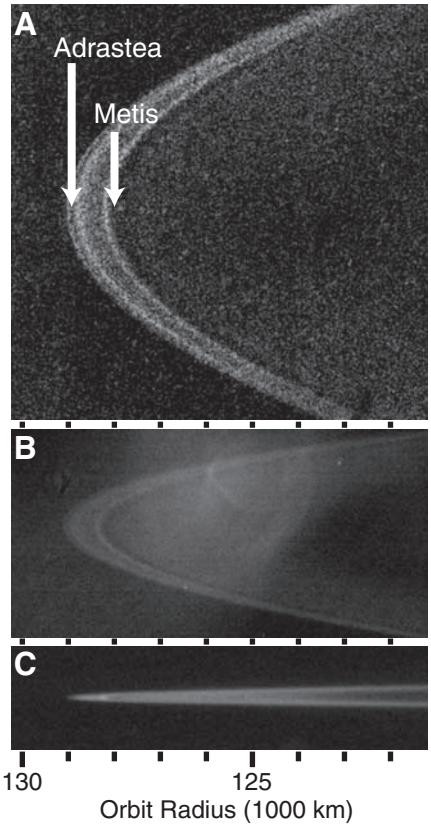

Fig. 1. The radial structure of the jovian ring in backscattered light (**A**) and forward-scattered light (**B** and **C**). Images are aligned vertically and shown at the same scale, as indicated by the horizontal axis. Solar phase angles are 21° (A), 120° (B), and 140° (C). The dust interior to the main ring becomes progressively brighter as the phase angle increases. Some scattered light appears in the middle of (B).

[1]Search for Extraterrestrial Intelligence (SETI) Institute, Mountain View, CA 94043, USA. [2]NASA Headquarters, Washington, DC 20546, USA. [3]Applied Physics Laboratory, Johns Hopkins University, 11100 Johns Hopkins Road, Laurel, MD 20723, USA. [4]Southwest Research Institute, 1050 Walnut Street, Suite 300, Boulder, CO 80302, USA. [5]Synthsys-D, 1200 South Riverbend Court, Superior, CO 80027, USA. [6]NASA Ames Research Center, Moffett Field, CA 94035, USA.

*To whom correspondence should be addressed. E-mail: mshowalter@seti.org

Table 1. Clump and body orbits and photometry.

Clump or body	Longitude at epoch* (°)	Mean motion (°/day)	a (km)	Equivalent radius† (km)
Family α		1210.547 ± 0.017	128737.7 ± 1.2	
α1	124.004 ± 0.035	1210.571 ± 0.039	128736.0 ± 2.8	0.86
α3	120.340 ± 0.021	1210.532 ± 0.020	128738.8 ± 1.4	0.79
α4	118.550 ± 0.066	1210.631 ± 0.063	128731.8 ± 4.5	
Family β		1210.471 ± 0.032	128743.0 ± 2.2	
β1	305.937 ± 0.219	1210.148 ± 0.224	128765.9 ± 15.9	
β2	303.957 ± 0.030	1210.478 ± 0.032	128742.6 ± 2.3	0.95
Adrastea‡	135.0	1207.001 ± 0.001	128980.5 ± 0.1	8.2
Metis‡	250.1	1221.252 ± 0.001	127979.8 ± 0.1	21.7

*Epoch is Julian ephemeris date 2454156.5 (25 February 2007). Longitudes are measured from the ascending node of the ring plane on Earth's J2000 equator. †Defined as the radius of a solid body equal in brightness, assuming properties similar to those of Adrastea. ‡Longitude from this work; mean motion, a, and size from earlier data (*14*).

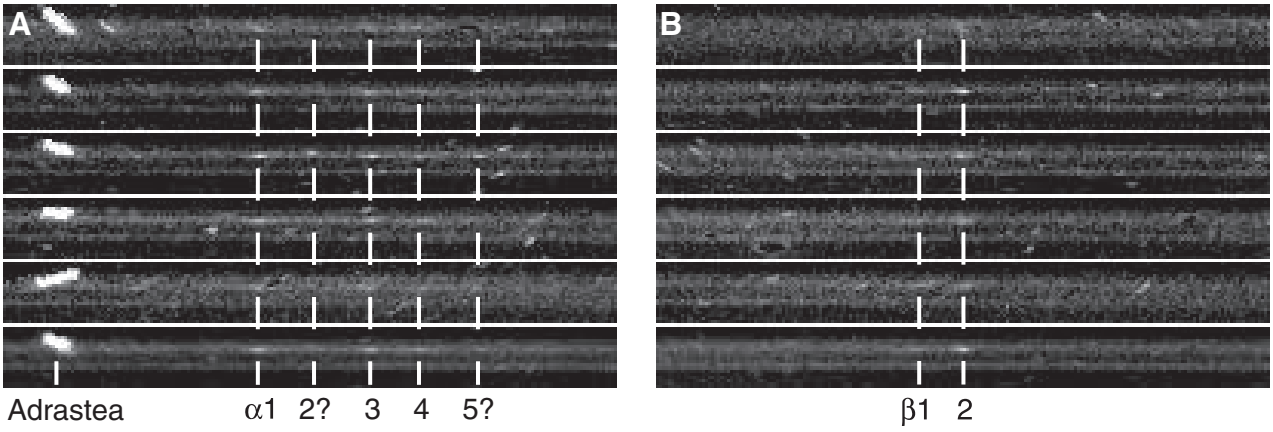

Fig. 2. Aligned image strips show the set of clumps identified as α (**A**) and β (**B**). Each strip has radial limits from 127,500 to 129,500 km. Longitudes are rotated to a common epoch, assuming the mean motion of a body at a = 129,000 km. Time steps increase upward. The bottom strip in each panel is an average of the strips above, which is used to show the clumps more clearly. Two of the five α features, numbered 2 and 5, are very marginal detections but seem to reveal an internal periodicity within this family.

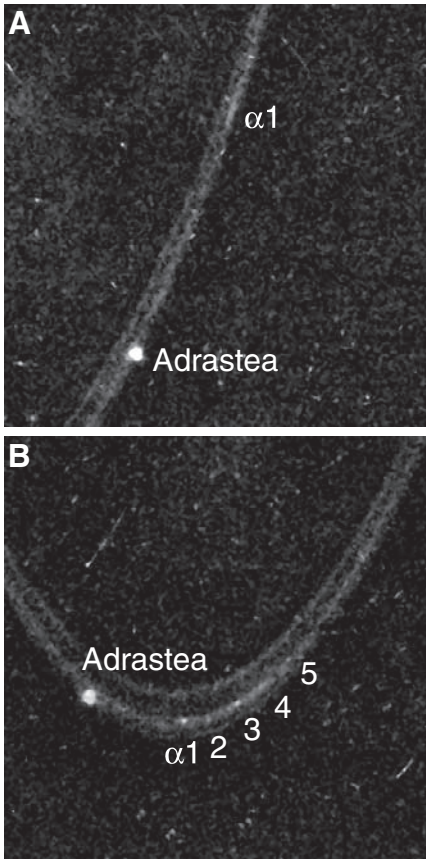

Fig. 3. Close-ups of feature α1 from images 34772943 (**A**) and 34774383 (**B**). The latter shows what appears to be a pointlike object near the tip of the ring, along with associated clumps α2 to α5. However, the longitude scale is less compressed as α1 approaches the tip (A), and it appears as an extended arc ~ 0.1° long.

using the mean motion for a body orbiting at the central radius of each strip. Thus, any object on a circular, equatorial orbit should appear aligned vertically at the same "rotating longitude" in adjacent strips and can be distinguished from the prevalent but randomly located background stars.

A set of unexpected features appeared (Fig. 2): two families of clumps within the main ring. Family "α" comprises three distinct features plus two more marginal ones; family "β" comprises two features separated by 2° in longitude. Both families are surrounded by a general brightening within several degrees of longitude. The clumps can be distinguished from moons because they have longitudinal extents ~ 0.1° to 0.3° (Fig. 3), which is larger than can be accounted for by image smear or resolution limits.

The brightest clumps are seen clearly in both ring movies, providing a time baseline sufficient to determine their orbits with reasonable precision (Table 1). The brightest features, designated

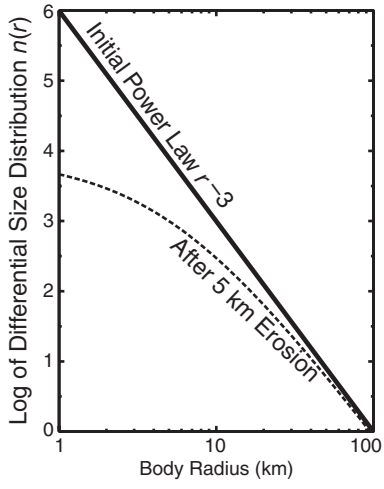

Fig. 4. An illustration of the effects of erosion on a power-law size distribution. Initially, bodies obey a differential size distribution $\propto r^{-3}$ (solid line). After erosion reduces all radii by 5 km, the population of smaller bodies (dashed line) is substantially reduced.

α1, α3, and β2, are two to three times as bright as the local ring, with integrated intensities ~1% that of Adrastea. If they are composed of material with similar albedo (5%), then each has a cross section that is equivalent to a moon ~1 km in radius. Based on the orbits, the clump families should have appeared repeatedly in outbound images taken a few days later, with phase angles 130° to 160°. The clumps are undetectable in these images, at sensitivity levels ~10% that of the main ring. Because the clumps are subtantially less forward-scattering than the main ring, they must be primarily concentrations of larger bodies, not dust.

No other moons or clumps were detected. The first ring movie was longitudinally complete between radial limits 104,000 to 185,000 km and was sensitive to moons 1 km in radius and larger. The second movie had narrower limits of 108,000 to 154,000 km and was sensitive to moons with r = 0.5 km. Our results reveal a marked truncation of the size distribution of moons in the inner jovian system. For comparison, until 2005, the smallest known regular satellite of Saturn was Calypso at r = 11 km. The Cassini mission has now revealed Daphnis at r = 6 to 8 km (*8*); Polydeuces, Pallene, and Methone each at r = 3 to 4 km (*9*); and Anthe (S/2007 S 4) at r ~ 1 km (*10*). Clearly, the population of saturnian moons shows no abrupt cutoff.

The large gap between 8-km Adrastea and our 0.5- to 1-km radius limit is therefore unexpected; it certainly violates our experience that astrophysical ensembles should follow power-law size distributions, with increasing numbers at smaller sizes. Two interpretations can be proposed. First, some models suggest that smaller bodies in planetary systems may have briefer lifetimes than larger ones against collisional disruption (*11*), although this assumes a steep size distribution of the incoming impactors. Alternatively, if micrometeoroid erosion plays an important role in the jovian ring (*2*), then this

process can act to truncate the size distribution. In erosive processes, dr/dt is a constant, independent of r. Hence, in the same time that Metis shrinks from $r = 27$ to 22 km, all 5-km bodies in the system would vanish (Fig. 4). This explanation requires that reaccretion be negligible, which is reasonable so deep inside Jupiter's Roche limit.

Earlier images from Voyager and Galileo showed longitudinal asymmetries on a scale much larger than the tiny clumps found by New Horizons (*6*, *7*, *12*). The absence such large features in the recent data is puzzling; perhaps seasonal or other time-scale variations play a role. Cassini images found one hint of smaller-scale clumping in the jovian ring (*13*). An arc ~ 8° in length appeared near the outer edge of the rings in three low-phase images, leading Adrastea at the time by ~4°. The epoch was ~0:00 UTC on 13 December 2000. We can extrapolate our clump motions backward for the intervening 2265 days to determine that features α and β fell 232° ± 39° and 226° ± 72° ahead of Adrastea (*14*). Unless unknown orbital perturbations are at work, these families can both be ruled out as the feature imaged by Cassini; apparently, that feature no longer exists. Cassini's images had lower resolution and SNR, however, so we cannot rule out α and β as long-lived features that were too small for Cassini to detect.

The presence of these clumps challenges our theoretical understanding. By Kepler shear, a 1-km-wide clump at α's orbit will spread 5.1° in 1 year; this distance is far larger than the few tenths of a degree of individual clumps. This leaves two alternatives: either the clump families are young or they are actively confined. Transient features could be explained by impacts from meteoroids or by collisions among the ring members. If the clumps are spreading, then this would provide an unambiguous indicator of their youth. Of the two clumps with best-determined orbits, α1 and α3 (Table 1), the leading clump appears to be moving slightly faster, suggesting that they might have emerged from a single point ~ 90 days before the flyby. However, the mean motions are too uncertain to rule out a much longer lifetime. Of course, a recent impact should generate substantial dust, such as is widely seen in Saturn's F ring (*15*–*18*), but Jupiter's clumps are not dusty. Also, an impact would be expected to produce one broad arc rather than the multiple, seemingly uniformly spaced clumps seen in the α family.

Alternatively, the 1.8° periodicity of clumps in group α is suggestive of a resonant confinement mechanism, perhaps comparable to Galatea's effects on the Adams ring of Neptune (*19*, *20*). Metis' resonances probably dominate; although it orbits three times as far away from the clumps as Adrastea, Metis is ~20 times more massive. Notably, Metis' 115:116 corotation inclination resonance falls at 128736.9 km, just 0.8 km from the orbit of the α family. Also, its adjacent 114:115 resonance falls at 128743.6 km, which is 0.6 km from the orbit of the β family. With 6.7 km between resonances, the probability that both families would fall so close to resonant locations by random chance is 4% (although the orbits have relatively larger uncertainties). However, these resonances are expected to confine material at intervals of ~ 180°/115 = 1.56°, which does not match the observed clump spacings. Nevertheless, the clumps in Neptune's Adams ring also do not show the predicted periodicities, suggesting that our understanding of resonant confinement remains incomplete.

The jovian ring's large-scale asymmetries have now vanished, but different, much smaller structures have been revealed. This follows upon observations that the radial structure of Saturn's equally faint D ring has changed radically in the past 25 years; some features have faded and spread, whereas other regions show entirely new structure (*21*). Similarly, the uranian ζ ring has recently been found to have shifted radially since the 1986 Voyager flyby (*22*). We conclude that the general class of dusty rings may be much more dynamic and time-variable than was previously supposed, with variations on 10- to 20-year time scales not the exception but the norm.

References and Notes

1. J. A. Burns, M. R. Showalter, J. N. Cuzzi, J. B. Pollack, *Icarus* **44**, 339 (1980).
2. J. A. Burns, M. R. Showalter, G. Morfill, in *Planetary Rings*, R. Greenberg, A. Brahic, Eds. (Univ. Arizona Press, Tucson, 1984), pp. 200–272.
3. J. A. Burns *et al.*, in *Jupiter: The Planet, Satellites and Magnetosphere*, F. Bagenal, T. E. Dowling, W. B. McKinnon, Eds. (Cambridge Univ. Press, Cambridge, 2004), pp. 241–262.
4. M. R. Showalter, J. A. Burns, I. de Pater, D. P. Hamilton, M. Horanyi, *Bull. Am. Astron. Soc.* **35**, #11.08 (2003).
5. I. de Pater *et al.*, *Icarus* **138**, 214 (1999).
6. M. R. Showalter, J. A. Burns, J. N. Cuzzi, J. B. Pollack, *Icarus* **69**, 458 (1987).
7. M. Ockert-Bell *et al.*, *Icarus* **138**, 188 (1999).
8. C. C. Porco, Cassini Imaging Team, *Int. Astron. Union Circ.* #8242 (2005).
9. J. N. Spitale, R. A. Jacobson, C. C. Porco, J. W. M. Owen, *Astron. J.* **132**, 692 (2006).
10. C. C. Porco, Cassini Imaging Team, *Int. Astron. Union Circ.* #8857 (2007).
11. R. M. Canup, L. W. Esposito, *Icarus* **113**, 331 (1995).
12. S. M. Brooks, L. W. Esposito, M. R. Showalter, H. B. Throop, *Icarus* **170**, 35 (2004).
13. H. B. Throop *et al.*, *Icarus* **172**, 59 (2004).
14. C. C. Porco *et al.*, *Science* **299**, 1541 (2003).
15. M. R. Showalter, *Science* **282**, 1099 (1998).
16. M. R. Showalter, *Icarus* **171**, 356 (2004).
17. J. M. Barbara, L. W. Esposito, *Icarus* **160**, 161 (2002).
18. S. Charnoz *et al.*, *Science* **310**, 1300 (2005).
19. C. C. Porco, *Bull. Am. Astron. Soc.* **22**, #1043 (1990).
20. F. Namouni, C. C. Porco, *Nature* **417**, 45 (2002).
21. M. M. Hedman *et al.*, *Icarus* **188**, 89 (2007).
22. I. de Pater, H. B. Hammel, M. R. Showalter, M. A. van Dam, *Science* **317**, 1888 (2007).

23. We thank the entire New Horizons mission team and our colleagues on the New Horizons science team. New Horizons is funded by NASA, whose financial support we acknowledge.

11 July 2007; accepted 19 September 2007
10.1126/science.1147647

REPORT

New Horizons Mapping of Europa and Ganymede

W. M. Grundy,[1*] B. J. Buratti,[2] A. F. Cheng,[3] J. P. Emery,[4] A. Lunsford,[5] W. B. McKinnon,[6] J. M. Moore,[7] S. F. Newman,[2] C. B. Olkin,[8] D. C. Reuter,[5] P. M. Schenk,[9] J. R. Spencer,[8] S. A. Stern,[10] H. B. Throop,[8] H. A. Weaver,[3] and the New Horizons team

The New Horizons spacecraft observed Jupiter's icy satellites Europa and Ganymede during its flyby in February and March 2007 at visible and infrared wavelengths. Infrared spectral images map H_2O ice absorption and hydrated contaminants, bolstering the case for an exogenous source of Europa's "non-ice" surface material and filling large gaps in compositional maps of Ganymede's Jupiter-facing hemisphere. Visual wavelength images of Europa extend knowledge of its global pattern of arcuate troughs and show that its surface scatters light more isotropically than other icy satellites.

NASA's Voyager and Galileo space probes revealed the icy Galilean satellites to be distinct, complex worlds with surfaces geologically and chemically sculpted by diverse endogenic and exogenic processes (*1*, *2*). Many outstanding questions remain regarding the composition and biological potential of Europa's interior ocean and the nature of its icy crust, the existence of possible oceans within Ganymede and Callisto, and the composition of enigmatic "non-ice" material on Europa and Ganymede that distorts their H_2O ice absorption bands (*3*–*5*).

During its 2007 flyby of Jupiter, New Horizons (*6*) observed Europa, Ganymede, and Callisto (table S1) with its infrared (1.25 to 2.5 μm) Linear Etalon Imaging Spectral Array (LEISA) (*7*) and its panchromatic (0.35 to 0.85 μm) LOng-Range Reconnaissance Imager (LORRI) charge-coupled device camera (*8*). LEISA observations used spacecraft motion to slew the field of view across